# Use of an octree-like geometry for 3-D dose calculations[a)]

D. L. McShan[b)] and B. A. Fraass
*Department of Radiation Oncology, University of Michigan Medical Center, Ann Arbor, Michigan 48109*

(Received 30 September 1992; accepted for publication 27 April 1993)

A representation used for 3-D graphical objects, the "octree," has been applied to the geometrical calculations needed to perform photon beam dose calculations for radiotherapy treatment planning. This representation allows the algorithm to attempt to minimize the number of distinct geometrical calculations that are needed to perform dose calculations to a particular resolution. In this way, the calculational time can be minimized, since the geometrical part of the dose calculations is often the most time-intensive part of the calculation process. The octree-like system used here has sped up the photon dose calculations described here by up to a factor of 10.

Key words: 3-D treatment planning, divergent geometry, dose calculations, photon beams, electron beams, pencil beams, dosimetric verification

## I. INTRODUCTION

One of the most time-intensive parts of photon dose calculations used for 3-D treatment planning is the calculation of geometrical parameters used in the 3-D dose calculations. These parameters include patient-related parameters like the source-surface distance (SSD) and depth inside the patient, as well as beam-related parameters like the location of a calculation point with respect to the shape and location of the radiation field. In many dose calculation models, the calculation of the SSD, depth, and location inside the beam ("the geometrical calculations") of all the calculation points can account for more than 90% of the time required for the 3-D dose calculations, particularly when the 3-D geometry of the patient and beam are taken into account.[1]

A number of different approaches to these geometrical calculations have been published. Siddon has discussed in detail some methodologies that can improve the speed with which standard ray-tracing geometrical calculations can be performed.[2] Starkschall has used different representations of the anatomical data to speed up the geometrical part of the dose calculations.[3] Yet another approach based on an octree-like representation has been described by Kooy,[4] and has been used in the context of electron pencil beam calculations.[5]

In the present work, we describe an approach to the geometrical calculations for 3-D dose calculations based on the use of an "octree-like" data structure to represent the geometry of the beam. The octree name was chosen because the representation used here is modeled after the octree approach to describing a volumetric object,[6,7] modified to account for the divergent beam geometry, which is used for dosimetric calculations. The data structures make use of a variable grid–type approach to the geometrical calculations to improve the efficiency of the calculations. The octree-like concepts are applied to the calculation of (1) the depth and SSD to each calculation point, and (2) the position of each point with respect to the beam.

This method has been part of the clinically used photon calculation algorithm[8] in the U-MPlan 3-D treatment planning system[9–11] since 1987. It has resulted in calculation time improvements of nearly a factor of 10 over the standard ray-tracing geometry calculations that were used previously. It has been designed for use with any photon or electron calculation model.

## II. MATERIALS AND METHODS

The work described here has been performed during the development of fast 3-D photon and electron calculation algorithms for the 3-D treatment planning system developed in our department. This planning system ("U-MPlan") has been described elsewhere,[9–16] and has been used for all clinical treatment planning in our department since early 1986. The software has been developed and used on DEC Vax computers, using FORTRAN. Current hardware platforms include a VAXCluster based with a VAX 8820, VAX 8700, and a number of VAXStation 3100 and 4000/90 workstations.

The objects used to define the patient anatomy[10,14] are briefly described here, since they are relevant to the geometrical calculations that are the subject of this work. All anatomical objects used in the system are three-dimensional.

*Structure.* A structure is a 3-D anatomical object. It can affect the 3-D density grid, which is used for dose calculations (external, inhomogeneity, and bolus types), or not affect dose calculations (internal structure type).

*Cut.* Cuts are 2-D planes of arbitrary orientation that typically coincide with CT scans or other imaging studies.

*Contour.* Contours are outlines drawn on cuts that describe the shape of a particular structure on a particular cut. The contours from a particular structure are meshed into a surface description, which is used for 3-D definition of the structure.

*Surface.* A surface is a 3-D surface description of a structure, created from multiple contours.

*Density grid.* A 3-D density grid is generated from the CT data (or alternatively, from manually defined contours and assigned densities), and the 3-D surface description of the external surface of the patient.

 0094-2405/93/20(4)/1219/9/$1.20  

## III. THEORY AND IMPLEMENTATION

### A. Octree concepts

An "octree" is a structure used to describe a volumetric object while minimizing the amount of space needed to contain the description. One begins with a cube containing the object to be described, and then subdivides it into eight equal cubes. If any of those cubes are empty (not containing the object), then that cube is removed from further subdivisions. The cubes that contain the object are then subdivided again and again, and cubes that do not contain any of the object removed from the subdivisions. This subdivision procedure continues until the desired resolution is reached. The resolution of the entire description is thus high where precision is needed, but large uninvolved areas do not take up large amounts of space in the description.

The application of this kind of "octree-like" concept to the geometrical calculations for radiotherapy dose calculations can deal with a number of the important issues in the calculation algorithm. First, there is a need for excellent precision and resolution in the calculation of geometry in some areas of the radiation field (i.e., near the field and block edges where there are large gradients in the dose distribution), but such precision is unnecessary where the dose distribution is fairly flat. The same concept applies to the calculation of distance and depth inside the patient: Where the surface curvature of the patient (with respect to the divergent fan lines radiating from the source of radiation) is flat, the resolution of the geometry calculations can be fairly large (at least in the across-the-beam directions), but when the surface has sharp irregularities, much finer resolution will be necessary.

### B. Geometrical calculations for radiotherapy dose calculations

The first kind of geometrical calculation necessary for most dose calculation algorithms is the calculation of the SSD and depth to an arbitrary point inside the patient. As illustrated in Fig. 1, this is a complicated calculation when including 3-D beam divergence and a 3-D description of the patient. In brute force methodologies, this calculation must be performed for each point included in the calculational grid. In our clinical practice, we find that it is not atypical to use a 3-D calculation point grid with 0.5-cm spacing between points over the volume of interest, resulting in from 300 000 to nearly 2 000 000 calculation points. In this situation, independent calculations of SSD and depth to each of these points can be extremely time intensive. For each SSD calculation, an algorithm must search over the entire 3-D surface description to find surface tiles that intersect with the ray, and then must calculate the intersection of the ray with the tile. Further ray-tracing calculations are required to determine the depth of the point inside the surface, especially if the radiological path length is required in order to perform density-corrected dose calculations.

The second kind of calculation needed determines the location of each calculation point with respect to the beam. In particular, one must determine the location of the point

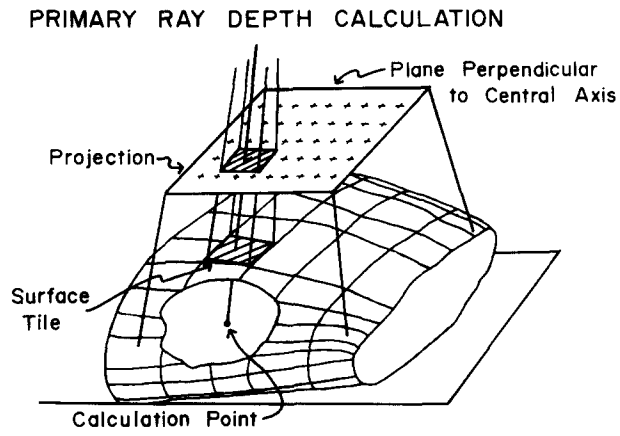


FIG. 1. Schematic illustration of the geometry involved in the primary ray depth calculation. A divergent beam ray is incident on the 3-D patient surface description (tiled). Also shown is a plane perpendicular to the beam central ray that is used to define the rays and other structures in the divergent geometry.

in the beam coordinate system that is tied to the treatment machine collimation system. Distance from the source of radiation is used for the inverse square law, as well as determining the relative location of the point with respect to the diverging beam edges. For calculation models that use off-axis ratios or other similar functions, the distance from the beam central axis must be known. Other models, such as the Edge model,[8,17] require the location of the point with respect to all of the beam geometry, in particular, the beam and block edges.

### C. Octree data structures

In order to apply octree-like concepts to the two geometrical problems described above, the geometry of the radiation beam is implemented in an octree-like way. As illustrated in Fig. 2, the beam is represented by a series of fan beams, called "rays." The beam is initially divided into $32 \times 32$ rays, extending 5 cm outside the beam edge in each

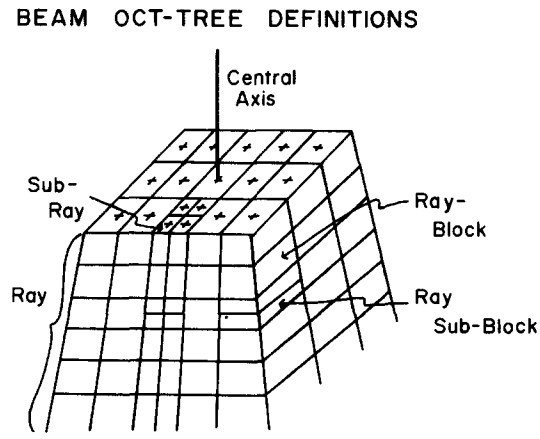


FIG. 2. Beam octree definitions are illustrated. The divergent beam geometry is divided into a quadtree (across the beam), and then the rays are divided into blocks. Rays and blocks both get subdivided as discussed in the text.

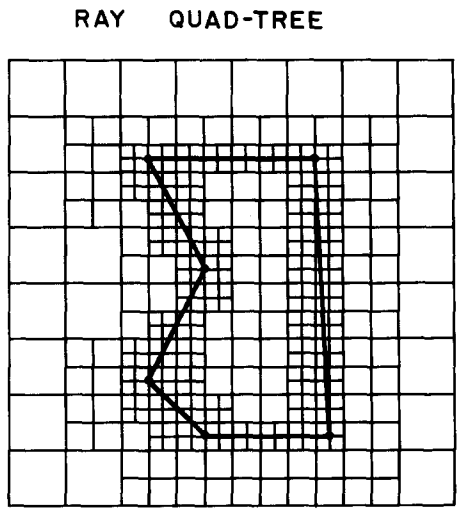


FIG. 3. View of the plane used for definition of divergent beam rays (plane is perpendicular to the beam central axis). Subdivisions of the coarse rays are generated whenever the coarse rays are near to a beam or block edge.

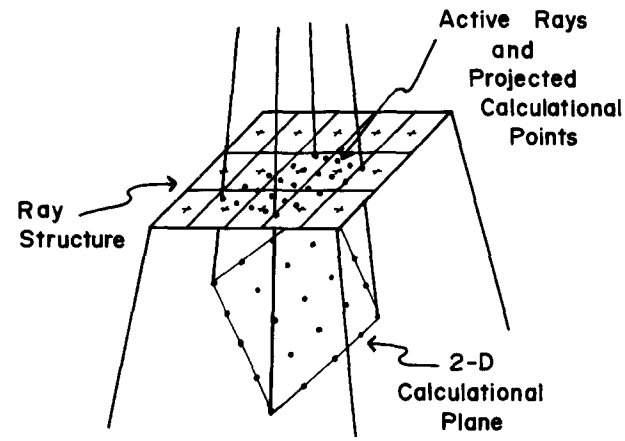


FIG. 4. Projection of calculation points into ray structure is illustrated using an oblique 2-D calculation plane. The points generated from a rectilinear grid tied to the oblique cut are divergently projected back into the ray structure, which is defined in the BEV plane (plane perpendicular to the beam central axis).

direction. Therefore, the resolution of the "coarse rays" in the "isocentric plane" (the plane perpendicular to the beam central axis that contains the isocenter of the beam) is between 1 and 1.5 cm, depending on the field size.

The most important features of the beam that must be handled with better resolution than the size of the original coarse rays are points near beam and block edges. Therefore, an octree-like subdivision of the rays is performed, based on the distance of the center of the ray from all the block, field, and patient edges [edge of the patient as seen in a beam's eye view (BEV) display]. This subdivision can be carried out to any resolution, based on a parameter MAXSUB, which limits the number of subdivisions, as well as parameters RAYSUB1,RAYSUB2,...,RAYSUB$n$, which determine the distance from an edge at which the $N$th subdivision will take place. For reference, our present clinical parameterization uses five subdivisions, with distance limits from 4 cm (for the first subdivision) to 0.5 cm for the last (fifth). This subdivision scheme is illustrated in Fig. 3. It results in a typical resolution of less than 1 mm between rays. Recently, subdivisions have been limited to those beam and/or block edges that define large ($>10\%$) differences in intensity. This change has negligible effect on the accuracy of the dose calculations, but decreases the octree calculation times by about a third for heavily blocked fields (for example, the field to be shown in Fig. 5).

In general, the subdivision of rays should also be based on the gradient of the patient external surface. However, knowledge of this gradient is not a simple calculation, like that of finding the distance from each ray center to beam and block edges. Therefore, in our current implementation, the only patient shape feature that affects the ray subdivision is the edge of the patient. The external surface is viewed in a beam's eye view geometry, and the edge of the patient in that view is treated just like the beam and block edges. Therefore, the rays are subdivided when they are near the edge of the patient surface. A more general patient-surface-gradient-based subdivision algorithm is possible, but has not yet been implemented.

For all calculation points contained in a particular ray, the calculation of the ray's location in the beam, and the SSD to the patient, are performed only once. However, not all rays need be calculated, since only those rays that contain points from the desired calculation grid may need to be considered. Typically, the calculation points are defined as a rectilinear grid of points defined with respect to the patient anatomy, although the use of randomly assigned points is also supported. The rectilinear grid points may be a volumetric grid of points, points aligned on one or more 2-D cuts, or lines or points anywhere in 3-D space. (See Fig. 4.) The dose for each of these points is calculated for each beam, and then the dose from each beam is summed to give the total dose to each point.

In order to determine which rays will contain calculation points, the points are projected onto the isocentric plane using the divergent beam geometry, as illustrated in Fig. 3. Points are then assigned to the ray in which they fall. Rays which do not contain any calculation points are removed from further calculations (unless the calculation model requires them). Since many calculation algorithms (including the Edge model[17]) only need to calculate distances and depths to specific calculation points, for many kinds of calculations a large number of rays may be bypassed, saving a great deal of calculation time.

The present work also uses a subdivision approach to the depth calculations which are needed. As shown in Fig. 2, after the ray subdivisions are determined, the rays are then broken up into depth "blocks." Large blocks are available for dose calculation models that have components of the dose calculation, such as the photon scatter, which are much more slowly varying than the primary attenuation.[18] The block size can be as large as 1 cm, but

TABLE I. Ray structure.

| Variable | Type | Description |
|---|---|---|
| LEVEL | Integer | Octree level (1=coarse) |
| FIRST_CALCPT | Integer | Pointer to first calculation point in this ray |
| CALCPT_COUNT | Integer | # of calculation points in this ray |
| FIRST_BLOCK | Integer | Pointer to first block in this ray |
| BLOCK_COUNT | Integer | # of blocks in this ray |
| SUB_RAY(4) | Integer array | Pointer to daughter rays subdivided from this ray |
| COARSE_RAY | Integer | Pointer to parent coarse ray |
| BACK_RAY | Integer | Pointer back to parent ray |
| RAYSECANT | Real | Secant of divergence angle for this ray, used to calculate the ray-line distance. RAYSECANT=SQRT(1+(RADIUS/SAD)**2) |
| RADIUS | Real | Radius from this ray to central axis at isocentric distance |

our implementation uses 0.5 cm. For quickly varying parameters, these depth blocks are subdivided into "subblocks." In our current parameterization, these subblocks have a resolution of 0.2 cm, and are used for most of the depth-related parameters in the edge model.[17] Since the depth blocks are created and subdivided with a different resolution than the rays, this data structure is not a true octree, or even an octree applied within the divergent geometry.

As with the projection of the rectilinear calculation points into the ray structure, the calculation points are also placed into these blocks and subblocks. All calculations are done only once for all points in a subblock. Therefore, if a subblock resolution of 0.2 cm is used, then all depth values used for points will be known with a resolution of 2 mm. This resolution has been judged to be adequate for photon dose calculation algorithms (2 mm will correspond to less than 0.5% for linear accelerators, except in the surface region), but would not be appropriate for an electron algorithm, where a 2-mm difference in depth may be quite important on the steep part of the depth dose curve. It is also expected that the accuracy of patient shape determination is not significantly better than this 2-mm resolution. However, if desired, this parameter may be changed to allow higher resolution subblocks.

In summary, then, the octree-like algorithm presented here provides the following geometrical information, which can be used by any calculation algorithm: (1) ray locations in beam coordinates, SSD to the patient surface for the center of the ray, and reference to the blocks and calculation points that are contained in those rays; (2) SSD and depth to each depth block contained in a ray, reference to the calculation points contained in the block, and the intensity and average density in each block; and (3) SSD, depth, and many other geometrical quantities, for each calculation point.

The ray, block, and point data structures are listed in Tables I–III, respectively. The ray structure describes all of the features of the rays. Note that for all the points included in each ray, the location of the ray with respect to the beam coordinate system is calculated only once (in the divergent beam coordinate system), rather than for each point. Each ray contains a number of blocks, each of which may contain a number of points. The block structure contains much of the depth information, including the current beam intensity and average density for each block. Finally, the point data structure contains the identifying information about each calculational point. The dose obtained at each point is included in that data structure. In order to decrease memory requirements, and to increase calculation

TABLE II. Block structure.

| Variable | Type | Description |
|---|---|---|
| IRAY | Integer | Index for parent ray |
| IYINDEX | Integer | Index for parent coarse ray |
| FIRST_CALCPT | Integer | Pointer to first point in this block |
| CALCPT_COUNT | Integer | # if points in this block |
| COARSE_BLOCK | Integer | Pointer to parent coarse block |
| BACK_BLOCK | Integer | Pointer to parent block |
| SUB_BLOCK(4) | Integer array | Array of pointers to daughter blocks |
| NEXT_BLOCK | Integer | Pointer to next block in ray chain |
| IYRAY_COARSE | Integer | Depth index (geometrical depth) |
| IYRAY_COARSE_EFF | Integer | Depth index (radiological path length) |
| YBEAM | Real | Central axis depth, relative to SAD, for block center |
| RAYDEPTH | Real | Depth of block (geometric) along ray |
| RAYDEPTH_EFF | Real | Effective depth (radiological path length) along ray |
| INTENSITY | Real | Beam fluence at this block |
| DENSITY | Real | Average density in this block |

TABLE III. Point structure.

| Variable | Type | Description |
|---|---|---|
| XCALC | Real | $X$ coordinate of point in TRS |
| YCALC | Real | Point $Y$ coord in TRS |
| ZCALC | Real | Point $Z$ coord in TRS |
| XBEAM | Real | Transverse coord (Beam Ref. System (BRS)) |
| YBEAM | Real | Distance along central axis relative to SAD plane, BRS coords |
| ZBEAM | Real | Longitudinal coord. (BRS) |
| XBEAM_SAD | Real | Ray-line intercept (transverse) at SAD (isocentric distance) |
| ZBEAM_SAD | Real | Long. ray-line intercept at SAD |
| RADIUS | Real | Radius of point from central axis (at SAD) |
| YENTRANCE | Real | Distance to skin entrance point |
| RAYDEPTH | Real | Ray-line depth to point |
| RAYDEPTH_EFF | Real | Radiological ray-line depth to point |
| NEXT_CALCPT | Integer | Pointer to next point in ray |
| RAY_COARSE | Integer | Pointer to parent coarse ray |
| RAY_FINE | Integer | Pointer to parent ray |
| IYRAY_COARSE | Integer | Coarse ray depth index |
| BLOCK_COARSE | Integer | Pointer to coarse block |
| BLOCK_FINE | Integer | Pointer to block |
| IYRAY_FINE_EFF | Integer | Index for effective (radiological) depth |
| IYRAY_FINE | Integer | Index for geometrical depth |
| DOSE | Real | Dose calculated to this point for this beam |

speed, these objects are chained together rather than being organized in a simple array of variables. The current limits for these structures are for points, 100 000; for blocks, 50 000; and for rays, 50 000. Since many more than 100 000 points are often required, the octree geometry calculation cycles through groups of 100 000 points in one pass, then performs the calculation for the next 100 000 points.

### D. Operational procedures

A summary of the differences between a standard approach to the geometrical calculations and the approach used here is given in Table IV. The basic calculational procedure used for geometry calculations is described in a step-by-step fashion below.

(1) Points are placed in the octree point data structure (the current implementation limits the number of points to 100 000 per cycle). Each rectilinear calculation grid point (or any other calculation point used to sum beam dose contributions) is used to create an entry into the octree point array. Points that exist in a region with electron density less than 0.05, or outside the external surface of the patient (density forced to be zero) are excluded from further calculations by removing the subblock from further operations.

(2) Coarse rays are created ($32\times32$) over the entire extent of the beam.

(3) Rays are subdivided where necessary. Beam coordinates of each ray are calculated once per ray.

(4) Points are projected into the ray structure, ordered in each ray, and then chained together. The chaining algorithm uses pointers to chain the points together in order to improve the efficiency of the array storage, as well as the speed with which the algorithm can find and scan over points contained in a particular block or ray.

(5) Blocks are created, and points are placed into the appropriate blocks.

(6) Blocks are subdivided where necessary.

(7) SSD and depth calculations are performed for all rays and blocks that contain points.

(8) Geometrical data is now stored in octree data structures, for use by the desired dose calculation algorithm.

(9) After the dose calculation is completed, move points (with dose included) back from octree data structures into the calculation point structures, which are used to sum individual beam contributions into a total dose distribution.

(10) If more than 100 000 points are to be calculated, return to (1) above and input the next set of 100 000 points into the octree point structure.

As discussed in Sec. IV, there is some overhead associated with all of the steps listed above. However, the efficiency of the algorithm is very good in the most commonly

TABLE IV. Differences between octree and standard geometry calculations.

| Conventional geometry | Octree geometry |
|---|---|
| Fixed rectangular grid | Fan beam grid |
| Each calc. point treated independently | Calculations grouped by fan rays |
| Inhomogeneity calculations slow (ray tracing to random points) | Inhomogeneity calculations faster (ray tracing organized by fan rays) |
| Scatter corrections slow (integration) | Possibility of scatter corrections with large resolution blocks |
| Difficult to vectorize | Data structures vector oriented |

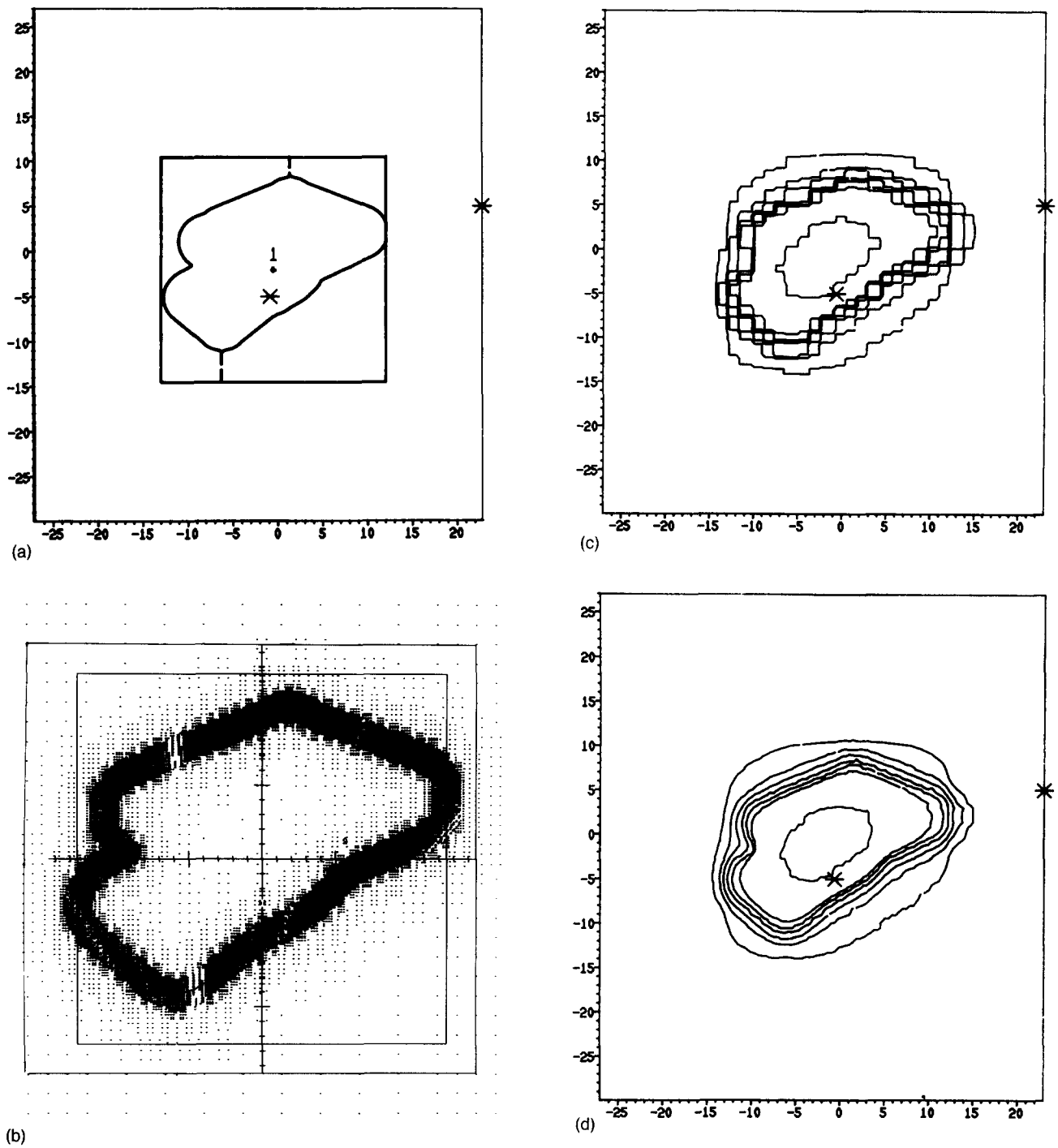


FIG. 5. Effects of octree resolution are demonstrated using a typical blocked field. (a) BEV display of field used for demonstration. Square collimator edges are shown, as well as block edges designed automatically (Ref. 11) to form a margin around the target volume (structure in center of figure). (b) BEV display with the actual center points of the rays highlighted. A 3-D grid of dose calculation points was used as the basis of the generation of this ray distribution. There are some asymmetries in the ray distribution due to anti-aliasing of the octree rays with respect to the rectilinear calculation grid points. (c) Dose calculation in a coronal plane for the field shown in panels (a) and (b), with all subdivisions of the octree turned off. Isodose lines shown are the 10%, 20%, 50%, 80%, 90%, and 98% isodose lines. (d) Same situation as panel (c), with the normal five subdivisions of the octree formalism turned on. The same isodose lines are displayed here as in panel (c).

used kinds of situations, including multiplanar and full 3-D calculations.

## IV. RESULTS

The result of the application of the octree methodology to photon dose calculations is illustrated here with a series of figures for a particular blocked field. Figure 5 shows a beam's eye view (BEV) display of a photon field with a number of shielding blocks. In Fig. 5(a), the desired field and block outlines are shown. Figure 5(b) is a diagnostic display available inside the planning system, which shows the center point of each of the rays used for this calculation. Note that the levels of subdivision are clear as one follows the beam/block edges around the field. Figure 5(c)

TABLE V. Illustration of calculation time saved. Calculational situation: prostate treatment, 2-D plane calculation, calculation point grid: 40×50, six field photon beam calculation, two conformal blocks in each field, inhomogeneity correction On, VAX 8820.

| Geometry used for calculation | Calculation time (s) |
|---|---|
| Conventional geometry | 180 |
| Octree geometry (0 subdivisions) | 18 |
| Octree geometry (3 subdivisions) | 20 |

TABLE VI. Resolution with octree-based calculations.

| Structure | Type | Resolution (cm) |
|---|---|---|
| Rays | Coarse rays | 1–1.5 |
| | Rays | 0.1 (with five add'l subdivisions) |
| Blocks | Coarse blocks | 0.5 |
| | Blocks | 0.2 |
| Points | Points | 0.2[a] |

[a]Resolution of depth, radiological depth, and SSD for each point.

shows the dose calculation that results when all of the subdivisions are prevented, so that the geometry of the calculation is performed with a resolution of more than 1 cm. Note that although it is clear that this resolution is not adequate for the calculation of primary-related effects, it may be reasonable for photon scatter-related effects. Figure 5(d) illustrates the dose distribution calculated with the usual octree parameters (five subdivisions), so that the final resolution near beam/block edges is about 1 mm. Note that in the center of the field where the dose distribution is fairly flat, the doses are not changed by the change in the subdivisions allowed.

One of the major reasons for the creation of the octree-based formalism is that the method should make possible a significant improvement in the speed with which many calculations are performed. The first example of the kind of improvement possible is shown in Table V. This simple single slice test case demonstrates nearly a factor of 10 improvement in the speed of the entire dose calculation. Note also that the time change for the addition of more subdivisions of the rays is quite small.

Analysis of the time required for the various parts of the algorithm has been studied for a number of different situations. One such situation is illustrated in Fig. 6, with the time required for various parts of the algorithm plotted against the number of points being calculated. Note that several parts of the process contain simple overhead tasks (creating finely spaced arrays so that individually calculated functions need not be calculated continuously, for example). The largest part of the calculation time (for the geometrical parts of the calculation, at least) is still the SSD/depth calculations, which are performed once for each ray that contains calculation points. The total calculation time is also greatly affected by the number and shape of blocks used in the field. As the complexity of the block shapes increase, there are many more rays near enough to a block edge that they will be subdivided, so the octree calculation times increase. This is to be expected, however, since as one gets more and more subdivisions in the octree to deal with more and more high resolution information, the time savings of the octree approach begins to tend toward the original time required by the brute force one-point-at-a-time method.

Finally, Table VI contains a summary of the geometric resolutions involved in the present configuration of the octree methodology. Note that all depth and SSD-related calculations are performed with a resolution of better than 2 mm, while the beam coordinate positions of points are known with varying resolution: Maximum grid size is 1.5 cm, while the minimum is about 1 mm.

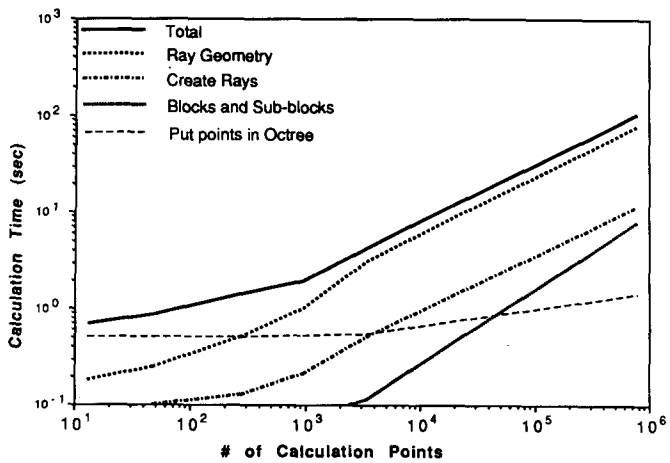


FIG. 6. Time spent for parts of the octree geometry calculation versus number of calculation points. These calculations performed on VAX 8820. These comparisons are dependent on the details of the experiment, but the curves shown here do illustrate the relationships between the various parts of the algorithm.

## V. DISCUSSION AND CONCLUSIONS

The use of octree-based geometrical calculations has made a significant contribution to the clinical usefulness of the 3-D treatment planning system developed in our institution. The increase in speed for the photon dose calculations can be as much as a factor of 10 over the one-point-at-a-time geometrical calculations used previously. As shown in the figures above, the time savings depends on the calculational situation: the largest time savings occur in the simple situations (axial cuts with axial beams and/or relatively simple blocking), but the octree algorithm is never slower than the comparable point by point method.

The octree methodology, as discussed in this work, allows the tailoring of the geometrical calculation resolutions to the specific problem at hand. Implementation of a primary plus scatter type of algorithm[18] could easily utilize the fine resolution information in the data structures for the primary calculation (where good resolution is needed), but could use the coarse ray and coarse block information for the scatter calculation, where the function varies slowly in space. Even with the use of the Edge model, the param-

eters determining the range and amount of subdivisions can be changed, so that the user may vary the resolution of the calculations if that is desired.

As mentioned earlier, the use of an octree representation has been discussed by Kooy and Kijewski,[4] and has been implemented for use in an electron pencil beam algorithm by Kooy and Rashid.[5] The improvements in time necessary for calculations are also accomplished for the electron pencil beam algorithm, as they have shown. Although the octree implementation discussed by these authors is somewhat different than that described here, the point of this representation is the same—to provide calculational speed improvements by tuning the resolution of the various geometrical calculations, which are required by a particular calculation algorithm to the needs of a particular clinical situation.

Several improvements to the methodology for assigning and subdividing rays could improve the efficiency and/or accuracy of the geometrical calculations. Creation of a fast method that could determine the gradient of the patient surface and/or density gradients within the patient, so that it could be used to help subdivide rays near important features in the patient's anatomy, would help improve the accuracy of dose calculations near these features. A second area that would benefit from additional research would be to determine if better use of the existing features of the method is possible. For example, it might be possible, for a particular subset of treatment fields, to utilize a much smaller region of subdivisions, thereby speeding up the calculations significantly. A four-field box plan, for example, might be done with an appropriate amount of dose calculation accuracy, even with most of the subdivisions turned off, since the errors caused by that action would be spread over all parts of the dose calculation, rather than localized near one particular edge of the target volume.

A more extensive change would be to separate the SSD/depth calculation resolution from the beam location resolution. Fine resolution rays are necessary for SSD and depth calculations only when the surface contour of the patient or the internal density structure is changing rapidly. Fine resolution information about the location of the calculation points in the beam geometry is only necessary near beam/block edges, or for devices that modify the beam intensity (for example, some wedges change the intensity quickly enough that a fine resolution knowledge of beam coordinates is important in order to prevent a "stair-step" appearance to the wedged field dose distribution).

The concepts used in the octree method of volumetric representation have been applied to the beam-patient geometry calculations, which are used extensively for radiotherapy dose calculations. By utilizing ray subdivisions in a divergent beam geometry, and further subdivisions of the rays into blocks and subblocks with depth, a number of different resolutions of geometrical information are available to dose calculation algorithms. This model has been implemented for a relatively fast photon calculation model (Edge model[17]), and has demonstrated calculation time savings of up to a factor of 10 over a standard 3-D ray-tracing method. The Edge/octree photon calculation model, which uses the octree method discussed here for its geometrical calculations, has been used for clinical treatment planning since 1987, and is useful over the full range of calculation types from single points to full 3-D volumes. Further optimization and improvement of the efficiency of the methodology will be the subject of future work.

[a]Presented in part at the 1987 meeting of the American Association of Physicists in Medicine, Detroit, Michigan, August 1987.

[b]Send reprint requests to Daniel L. McShan, Ph.D., Department of Radiation Oncology, University of Michigan Medical Center, Room B2C490, Box 0010, 1500 E. Medical Center Dr., Ann Arbor, Michigan 48109-0010.

[1]B. A. Fraass and D. L. McShan, "Developments in radiation therapy treatment planning," in *Computers in Medical Physics*, edited by A. R. Benedetto, H. K. Huang, and D. P. Ragan (American Institute of Physics, Woodbury, NY, 1990), 303–315.

[2]R. L. Siddon, "Prism representation: A 3-D ray-tracing algorithm for radiotherapy applications," Phys. Med. Biol. **30**, 817–824 (1985).

[3]G. Starkschall, "Analytic evaluation of depths of dose calculation points for external beam radiation therapy treatment planning," Med. Phys. **12**, 477–479 (1985).

[4]H. M. Kooy and P. K. Kijewski, "Quadrees as a representation for irregularly shaped fields in radiotherapy applications," Int. J. Rad. Oncol. Biol. Phys. **15**, 1251–1256 (1988).

[5]H. M. Kooy and H. Rashid, "A three-dimensional electron pencil beam algorithm," Phys. Med. Biol. **34**, 229–243 (1989).

[6]D. Ayala, P. Brunet, R. Juan, and I. Navazo, "Object representation by means of nonminimal division quadtrees and octrees," ACM Trans. Graphics **4**, 41–59 (1985).

[7]J. Veenstra and N. Ahuja, "Line drawings of octree-represented objects," ACM Trans. Graphics **7**, 61–75 (1988).

[8]B. A. Fraass, D. L. McShan, R. K. Ten Haken, and K. M. Hutchins, "3-D treatment planning: V. A fast 3-D photon calculation model," in *The Use of Computers In Radiation Therapy*, edited by I. A. D. Bruinvis, P. H. van der Giessen, H. J. van Kleffens, and F. W. Wittkamper (Elsevier, Amsterdam, 1987), pp. 521–524.

[9]B. A. Fraass and D. L. McShan, "3-D treatment planning: I. Overview of a clinical planning system," in *The Use of Computers In Radiation Therapy*, edited by I. A. D. Bruinvis, P. H. van der Giessen, H. J. van Kleffens, and F. W. Wittkamper (Elsevier, Amsterdam, 1987), pp. 273–276.

[10]B. A. Fraass, D. L. McShan, R. F. Diaz, R. K. Ten Haken, A. Aisen, S. Gebarski, G. Glazer, and A. S. Lichter, "Integration of MRI into radiation therapy treatment planning," Int. J. Rad. Oncol. Biol. Phys. **13**, 1897–1908 (1987).

[11]D. L. McShan, B. A. Fraass, and A. S. Lichter, "Full integration of the beam's eye view concept in clinical treatment planning," Int. J. Rad. Oncol. Biol. Phys. **18**, 1485–1494 (1990).

[12]B. A Fraass, "Clinical utility of 3-D treatment planning," in *Advances in Radiation Oncology Physics: Dosimetry, Treatment Planning and Brachytherapy*, edited by J. A. Purdy (American Institute of Physics, Woodbury, NY, 1992), 967–997.

[13]B. A. Fraass, D. L. McShan, and K. J. Weeks, "3-D treatment planning: III. Complete beam's-eye-view planning capabilities," in *The Use of Computers In Radiation Therapy*, edited by I. A. D. Bruinvis, P. H. van der Giessen, H. J. van Kleffens, and F. W. Wittkamper (Elsevier, Amsterdam, 1987), pp. 193–196.

[14]D. L. McShan and B. A. Fraass, "3-D treatment planning: II. Integration of gray scale images and solid surface graphics," in *The Use of Computers In Radiation Therapy*, edited by I. A. D. Bruinvis, P. H. van der Giessen, H. J. van Kleffens, and F. W. Wittkamper (Elsevier, Amsterdam, 1987), pp. 41–44.

[15]D. L. McShan, R. K. Ten Haken, and B. A. Fraass, "3-D treatment planning: IV. Integrated brachytherapy treatment planning," in *The Use of Computers In Radiation Therapy*, edited by I. A. D. Bruinvis, P. H. van der Giessen, H. J. van Kleffens, and F. W. Wittkamper (Elsevier, Amsterdam, 1987), pp. 249–252.

[16]R. K. Ten Haken, R. F. Diaz, D. L. McShan, B. A. Fraass, J. A. Taren, and T. W. Hood, "Manual vs computerized planning and dosimetry for stereotactic brain implants," Int. J. Rad. Oncol. Biol. Phys. **15**, 467–480 (1988).

[17]B. A. Fraass, D. L. McShan, and M. K. Martel, "Fast photon beam

dose calculations with an edge-based calculation model," (submitted to Med. Phys.).

[18]M. R. Sontag, M. D. Altschuler, P. Bloch, R. A. Reynolds, R. E. Wallace, and G. K. Waxler, "Design and clinical implemementation of a second generation three-dimensional treatment planning system," in *The Use of Computers In Radiation Therapy*, edited by I. A. D. Bruinvis, P. H. van der Giessen, H. J. van Kleffens, and F. W. Wittkamper (Elsevier, Amsterdam, 1987), pp. 285–288.